

Alpha helical crossovers favor right-handed supersecondary structures by kinetic trapping: The phone cord effect in protein folding

Benjamin J. Cole^{1,2,3} and Christopher Bystroff^{1*}

¹Departments of Biology and Computer Science, Center for Biotechnology and Interdisciplinary Studies, Rensselaer Polytechnic Institute, Troy, New York 12180

²Plant Biology Laboratory, The Salk Institute for Biological Studies, 10010 North Torrey Pines Road, La Jolla, CA 92037

³Division of Biological Sciences, Section of Cell and Developmental Biology, University of California San Diego, La Jolla, CA 92093

Received 11 March 2009; Revised 11 May 2009; Accepted 21 May 2009

DOI: 10.1002/pro.182

Published online 8 June 2009 proteinscience.org

Abstract: The remarkable predominance of right-handedness in beta-alpha-beta helical crossovers has been previously explained in terms of thermodynamic stability and kinetic accessibility, but a different kinetic trapping mechanism may also play a role. If the beta-sheet contacts are made before the crossover helix is fully formed, and if the backbone angles of the folding helix follows the energetic pathway of least resistance, then the helix would impart a torque on the ends of the two strands. Such a torque would tear apart a left-handed conformation but hold together a right-handed one. Right-handed helical crossovers predominate even in all-alpha proteins, where previous explanations based on the preferred twist of the beta sheet do not apply. Using simple molecular simulations, we can reproduce the right-handed preference in beta-alpha-beta units, without imposing specific beta-strand geometry. The new kinetic trapping mechanism is dubbed the “phone cord effect” because it is reminiscent of the way a helical phone cord forms superhelices to relieve torsional stress. Kinetic trapping explains the presence of a right-handed superhelical preference in alpha helical crossovers and provides a possible folding mechanism for knotted proteins.

Keywords: protein folding; molecular simulations; Ramachandran plot; handedness

Introduction

Anyone who has ever coiled a rope knows that you have to twist the ends to get the coil to stay flat. Depending on which way you twist the ends, you get either a right-handed or a left-handed rope coil. We believe that the same can be said for an α -helix during protein folding—

that the ends of the helix must also twist. Coiling a rope creates torque on the ends because the rope cannot pivot to relieve torsional stress. A ball-chain (see Fig. 1) is an example of chain that can pivot freely, and this type of chain does not require twisting of the ends to form a helix. Because the polypeptide backbone contains rotatable bonds, it appears to be like a ball-chain. But the polypeptide backbone ϕ and ψ angles do not rotate freely; both must pass through disallowed regions of the Ramachandran plot. Because those barriers are high, a polypeptide chain is expected to behave partially like a rope—perhaps like the familiar coiled phone cord that allows but resists torsional stress. It follows that the formation of a helix should create torque on the ends. This torque may be relieved by the

Additional Supporting Information may be found in the online version of this article.

Grant sponsor: NSF (REU supplement); Grant numbers: DBI-0508703, DBI-0448072; Grant sponsor: The Howard Hughes Medical Institute.

*Correspondence to: Christopher Bystroff, Department of Biology, Rensselaer Polytechnic Institute, 110 8th St., Troy, NY 12180. E-mail: bystrc@rpi.edu

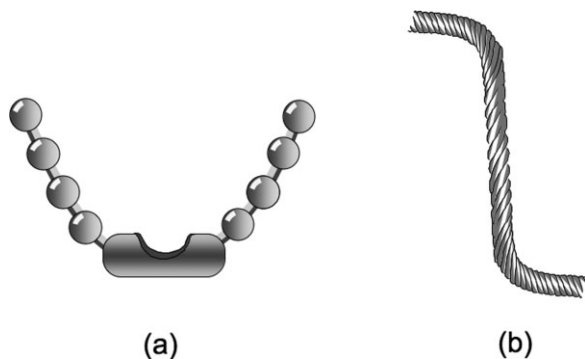


Figure 1. (a) A ball-chain is flexible and forms coils easily. (b) A rope is stiff and needs to be torqued to form a coil.

formation of helical supersecondary structures, such as $\beta\alpha\beta$ units and $\alpha\alpha\alpha$ three-helix bundles in protein structures.

The predominance of right-handed form of $\beta\alpha\beta$ units—supersecondary structure units containing a two-stranded parallel β sheet and a crossover α -helix—was noted in the 1970s when there were enough crystal structures to do statistics, and theories were proffered at the time,^{1,2} mostly founded on the observed right-handed twist of β sheets and β strands. This twist is itself a result of the homochirality of L-amino acids in proteins. These proposed origins of right-handedness can be summarized as follows. When a twisted β sheet is crossed by a helix in a right-handed manner, the helix lies along a straight line connecting the ends; when it is crossed in a left-handed manner, the helix must sit farther away from the line to accommodate the sheet, and the loops connecting the helix to the sheet must be concomitantly more extended. Chou *et al.* performed simulations of both right- and left-handed conformations and found that the molecular mechanics energy, primarily from torsion angles in the loops, was more favorable in the right-handed fold.³ They observed that the packing of the helix against the sheet in the left-handed form produced a flatter sheet containing a less favorable hydrogen bond geometry. This explanation made sense, because the more extended loops and helix would naturally have fewer conformational options in the longer left-handed crossover than in the shorter right-handed one.

Richardson,¹ on the other hand, recognized that right-handedness was preferred regardless of the length of the crossover segment and proposed a different explanation. Her hypothesis was that the slight right-handed twist of an extended poly-L-peptide chain led to a preference during folding of coming together with an overall right-handed topology. This would be true whether the crossover was an alpha helix or otherwise. This too makes sense. In fact, crossovers between parallel sheets in two sheet sandwich proteins are also predominantly right-handed. The twisted sheet hypothesis^{2,3} also explains the right-handedness of beta sandwiches.

Although these theories have gone almost unchallenged for decades, they leave much to be accounted for. Why, for instance, do $\beta\alpha\beta$ units that contain very long loops and multiple helices still maintain the same statistical predominance of the right-handed form? If the energetic argument was the sole explanation for right-handedness, one would expect a few of the longer, loopier crossovers to be left-handed, but this is rarely the case.

Why is the statistically preferred chirality of $\alpha\alpha\alpha$ three-helix crossovers, containing no β sheet, also right-handed? Unlike β -strand pairing, the packing of the two helices on the ends of a three-helix bundle cannot be said to have a preferred right-handed twist. In fact, the preferred packing of two helices might best be taken to be the left-handed supercoil of coiled-coil domains, which would argue for a preferred left-handed crossover.

Richardson's hypothesis of a strong preference during initial collapse does not explain the existence of both right-handed (e.g., alkaline protease subunit P, 1K7I_A) and left-handed (e.g., antifreeze protein, 1LOS_A) β -helix proteins—to be fair, structures not known at that time. According to Jenkins *et al.*,⁴ the discovery of the left-handed beta helix “challenged an almost 20 year dogma” of the thermodynamic preference for right-handed crossovers.

Here, we present another hypothesis for the origins of handedness in protein supersecondary structure, based on the dynamic nature of poly-L-peptides. If a polypeptide chain is like a phone cord, then in the process of forming a helix, it will generate torque on the flanking sequences. If the flanking sequences are in contact with each other before the helix is fully formed, then the torque generated by helix formation will either pull those contacts apart or push them together, depending on whether they are left-handed or right-handed contacts (see Fig. 2). Torque is dissipated by pulling left-handed contacts apart and rotating until right-handed contacts are made. Once the right-handed contacts are made, additional torque generated by helix formation can only be dissipated by crossing energetically unfavorable torsional barriers.

Using a demonstrative model, we simulate the formation of a helical crossover unit, showing that the torque generated by helix formation pulls apart contacts if the crossover is left-handed, and pushes them together if the crossover is right-handed. If so, then it would mean that right-handed crossovers are kinetically trapped during folding. The proposed folding phenomenon is exploited to explain the formation of knots in two knotted proteins.

Results

Topological analysis of three-helix bundles

In all, there were 431 three-helix bundles within all-alpha class protein that could confidently be assigned a handedness. Of these, 61.5% were right-handed, 38.5% left-handed. If no energetic difference existed

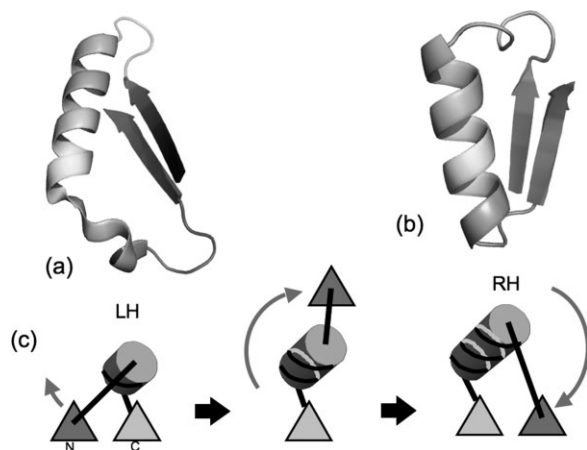


Figure 2. (a) 1J9L (123–165)—A left-handed beta-α-beta unit. These comprise ~1.5% of the structures in the nonredundant protein database. (b) 1BYS (57–87)—A right-handed beta-α-beta unit. These comprise ~98.5% of the structures in the nonredundant protein database. (c) TOPS diagram⁵ showing how torque applied to the ends of a nascent helix convert left-handed to right-handed. As the helix grows, the ends rotate. Triangles pointing up represent β-strands pointing out of the image.

between R and L, and sampling was representative, then the counts should have partitioned themselves evenly within statistical limits. However, the chance likelihood of getting $\geq 61.5\%$ right-handed out of 431, given the null hypothesis of equally likely R and L forms was $P = 0.0001$, determined using the resampling method.⁶ Thus, we can say with confidence that there is an unexplained preference for the right-handed topology in three-helix bundles. A complete listing of three-helix bundles is available as Supporting Information Table I.

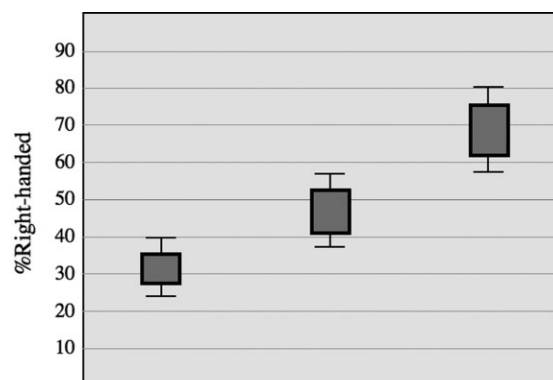
A statistical preference for right-handedness in three-helix bundles was also found if we selected all-alpha proteins at the SCOP “fold” level rather than at the superfamily level, but because of smaller sample size the statistical significance was not as great. Also, a similar statistical preference was found in these studies if a helix was redefined to be at least 5, 6, 7, or 8 residues in length, rather than at least four residues. Again statistical significance decreased because of smaller sample sizes.

Analysis of demonstrative molecular simulations

Supporting evidence for the “phone cord effect” hypothesis was sought using molecular simulations. The point was to demonstrate under controlled conditions the emergence of a preference for right-handed helical crossovers given only the assumption that an energetic barrier exists to the rotation of the Cα-carbonyl carbon bond at approximately $\psi = -120^\circ$. This barrier between α and β energy basins was found originally by Ramachandran using local steric interactions⁷ and is reflected in the statistics of backbone angles in high-resolution crystal structures.⁸ Conversions between

energy basins in molecular dynamics simulations, regardless of forcefield, are found to pass through the same regions that are statistically more populated in crystal structures.⁹ Therefore, it makes sense that lower database frequencies of backbone angles reflect higher energies, and that the higher frequency observed at around $\psi = 0$ when compared with $\psi = -120^\circ$ reflects a lower barrier for the southern route to helix. In this article, we will use the term “south” to refer to the rotation of ψ from extended to helix through zero, and “north” to refer to the rotation from extended to helix through $\psi = 180^\circ$.

In the experiment (all south) where the ψ angles for all of the H-segment residues were given a barrier at -120° , 69% of the simulations that folded successfully and had an unambiguous handedness were trapped in the right-handed form, 31% in the left-handed form. Also observed is an emergence of a left-handed preference in the experiment (All north) where the energy barrier in ψ was drawn at $\psi = 0$, forcing the ψ angles to travel north through 180° en route to helical angles. Thirty-one percent were trapped in the right-handed state, 69% in the left-handed. No significant handedness preference is observed in the experiment (50/50), where residues were randomly assigned an equal number of north and south barriers. The results are summarized in Figure 3.



Experiment	All North	50/50	All South
Trials	2738	1164	501
Collapsed	2540	1066	418
Helical	851	578	286
Ambiguous	456	299	131
Right-handed	124	130	107
Left-handed	271	149	48
%R-handed	31%	47%	69%

Figure 3. Results for three experiments using simplified molecular simulations. Trials: total simulations. Collapsed: trials ending with termini on the outside of floors. Helical: collapsed trials with at least five consecutive residues with helical $\phi\psi$ angles. Ambiguous: collapsed, helical trials where handedness was U according to Eq. (2). Right-handed: collapsed, helical trials where handedness was R. Left-handed: collapsed, helical trials where handedness was L. Boxes show 95% confidence, and bars show 99% confidence levels.

Discussion

Right-handedness in three-helix bundles

Clearly, the statistics for three-helix bundles are not as strong when compared with the 66:1 ratio of right- to left-handed $\beta\alpha\beta$ units. The additional handedness preference in $\beta\alpha\beta$ units may be the result of beta-sheet curvature, in accord with previous theories, or it could be the result of stickier contacts between two beta strands when compared with between two alpha helices. Stronger interactions would create a sharper energy landscape with higher barriers, more likely to trap the polypeptide in the crossover configuration, amplifying the proposed phone cord effect. Further, it has been shown experimentally that some well-studied three-helix bundles do not form the crossover contact early¹⁰ and would therefore not be trapped by the phone cord effect.

The reliability of these statistics depends on the quality of the data used. If the data were somehow oversampled in right-handed three-helix bundles for reasons other than energetic preference, then the statistical result would be suspect. Steps were taken to factor out homology as a source of overcounting. Proteins related by sequence or structural homology were first removed using SCOP,¹¹ a manually curated classification system for protein structures. In SCOP, each superfamily has been judged by experts to be a different fold, inferring independent evolutionary origins—any similarities in structure between superfamilies occur at the local, not global, level. We presume these similarities to be the results of convergent, not divergent, evolution. Convergent evolution is driven by energetic selection rather than by functional selective pressure. Therefore, significant differences in the frequency of substructures reflect on the relative energies of those substructures.

The application of database statistics to find recurrent structural themes in proteins and to infer energetic preferences is not new. Database statistics have been used previously to build knowledge-based potentials^{12,13} and to infer the locations of folding initiation sites.^{14,15} Energetic preferences in local structure inferred from database statistics have been corroborated by molecular dynamics simulations^{16,17} and by experimental structural studies,^{18,19} where the results are defined by energetics alone.

Handedness correlates with barrier position in molecular simulations

In these simulations, we drove the backbone angles from extended to helical using backbone torques, but in reality the energy landscape is more complex, captured only partly by the barriers to chain crossing. For the “all south” experiment, we found that in 286 of 418 simulations, the helix was mostly formed after 8000 time steps (68%), but in the “all north” simulations, only 851 of 2540 simulations had a mostly formed helix (34%). The formation of a helix via the

southern route may take place in a concerted way, whereas the northern route would force residues to “take turns” adjusting to helical angles. Concerted shifts to the north would produce a chain crossing (animations showing concerted helix formation via the south pathway and the north pathway are provided as Supporting Information.). As a result, more of the north simulations ended in a tangled mess that could not proceed. Further smoothing the way for the southern route, concerted consecutive southern shifts pass through 3–10 helix, where backbone oxygens and nitrogens are temporarily stabilized in i to $i + 3$ H-bonds on the way to a helix. The domination of the southern route in folding of real helices is likely greater than suggested by these simulations.

Chain crossing was prevented by hard sphere repulsion, and the crossover configuration was maintained using gravity, as described in Methods. But in many of the simulations, the B1 and B2 regions were seen to pass each other, not by chain crossing but by the act of one strand sliding through the space between the other strand and the helix. Many of the trials labeled as ambiguous were trapped in a state resembling folded arms, with one strand partially inserted under the other. This is unlikely to occur in a full-length protein unless the helix is close to one of the termini. This observation suggested one of the two ways that a knot could form in a protein. The correlation between north/south and left/right remains strong despite this leak-through, which must have a high entropic barrier.

How the phone cord effect could produce a knot

Topological knots are rare in proteins, because to form a knot, one end of the chain must thread its way through a loop in the chain, an entropically costly event. But what if there was a driving force behind the threading event? The rotating end of the helix as it forms might act as such a motor. If folding places it in the proper orientation with respect to a loop, then rotation of the end of the helix could drive it through.

To illustrate, consider the knotted protein *H influenza* methyltransferase (PDB code 1MXI). The protein is of the class α - β , specifically a 5-6-3 α - β - α three-layer sandwich, with six parallel β strands, arranged 645123, and 7 α helices. All crossovers helices are in the right-handed configuration. The C-terminal helix $\alpha 7$ forms a knot in the chain by passing through the $\beta 4$ - $\alpha 6$ - $\beta 5$ crossover unit. Mutational studies have shown that the formation of the knot is late in the folding process, and that the kinetics of folding are sensitive to mutations in the knotted region.²⁰ As a possible explanation for this deep trefoil knot, we propose that a late folding intermediate exists in which the positions of $\alpha 6$ and $\alpha 7$ are swapped and $\alpha 7$ is not yet a full-length helix. The N-terminal loop of $\alpha 7$, being very hydrophobic, may find its way into the space between $\alpha 6$ and

the β sheet. Continued folding of $\alpha 7$ would, according to the phone cord theory, cause a left-handed rotation of this hydrophobic loop, which would push $\alpha 6$ away from the β sheet and pull $\alpha 7$ through the loop. An illustration of the proposed pathway is provided as Supporting Information Figure 1.

The variable domain of human immunoglobulin kappa IV light chain (PDB code 1LVE chain I) contains a figure-8 knot, in which a long C-terminal tail is threaded through an extended loop made up of two α helices and a random coil region. The phone cord theory allows us to elaborate on a folding mechanism originally proposed by Taylor.²¹ Taylor noted the pseudosymmetry of the core helical elements in this all- α domain, suggestive of an ancient gene duplication event. The core helices were proposed to first become associated in an interlocked, yin-yang, four-helix bundle, early in folding. The knot could form if the collapse of the rest of the chain around the core happened in a specific order, with the C-terminal segment passing through the long central loop before the latter had folded. Here, we propose a non-native intermediate in which the central segment collapses around the four-helix bundle. After this event, the pair of C-terminal helices fold against the expanded core, trapping one half of the central segment. Then, formation of a helix in the central segment causes it to roll over the C-terminal segment, settling on the other side of the protein, and forming the knot. The rolling motion is driven not only by random diffusion but also by the phone cord effect, which drives the loop from a left-handed to a right-handed crossover. The loop rotation relieves some of the torque generated by helix formation. This folding pathway is illustrated in Supporting Information Figure 2.

Conclusions

Formation of superhelicity in proteins is viewed as an emergent phenomenon of the inherent stiffness of a polypeptide chain in combination with the formation of alpha helices during folding. When a helix forms in a stiff chain, it produces a net torque on the ends, which may be relieved by pivoting of the chain, or by rotation of one end of the chain. If the chain is in a crossover configuration when the helix forms, rotation of one end of the chain in a left-handed manner leads to a right-handed crossover. The result is a kinetic trapping mechanism for right-handed helical crossovers. In the case of $\beta\alpha\beta$ units, the preference from the kinetic trapping mechanism reinforces the well-known thermodynamic preference. However, we have shown an unexplained statistically significant over-representation of right-handedness in three-helix bundles, which would be explained by the phone cord effect but not by thermodynamic arguments. We have also demonstrated the emergence of handedness in bare-bones molecular simulations, requiring nothing more than the known rotational barriers in phi and psi. And, we

have exploited the phone cord effect as the driving force for molecular motions that would explain the formation of knots in two proteins.

Methods

Statistical analysis of three-helix bundle topology

Three-helix bundles are defined here as protein substructures containing three consecutive helices, with no intervening beta strands, in which the first and third helices are in close contact. Three-helix bundles can be either right- or left-handed. All three-helix bundles were extracted from the SCOP database (version 1.73),¹¹ using one representative from each all-alpha superfamily. Three-helix bundles also occur in mixed secondary structure proteins, but statistics were not taken from within α -beta class of proteins to avoid the causative role of beta sheets.

Helical segments within protein structures were identified using backbone angles. At least four consecutive residues were required to have ϕ and ψ angles in the range $(-60 \pm 60, -50 \pm 60)$.

The handedness, right (R) or left (L), of any three-helix bundle was determined to be

$$R \text{ if } (\vec{h} \otimes \vec{c}) \bullet \vec{n} > 0, \text{ otherwise } L \quad (1)$$

where h is a vector from the first to the last residue in the central helix, c is a vector from the first residue of the helix to a contact residue i , C-terminal to the helix, and n is a vector from the first residue of the helix to a contact residue j , N-terminal to the helix. Contact residues were any pair of C-alphas i and j with distance less than 7 Å. This method rarely fails to identify the correct handedness when such a handedness is unambiguous to the trained eye, but to be certain, we averaged the handedness value over all contact residues and kept only those three-helix bundles where the handedness was confidently assigned, as follows.

$$\text{if } \frac{\sum_{ij} R(i,j)}{N_{ij}} \begin{cases} > 0.75, & R \\ < 0.25, & L \\ \text{otherwise,} & U \end{cases} \quad (2)$$

where the value of $R(i,j)$ is 1 if the result of Eq. (1) using endpoints i,j is R, otherwise 0. Examples with ambiguous handedness (U) were not used.

A similar analysis was applied to all $\beta\alpha\beta$ units in the nonredundant PDBselect (Apr 2007) dataset of known structures,²² finding that 98.5% were right-handed and 1.5% left-handed, with a ratio of 66:1.

Algorithm for demonstrative molecular simulations

Internal coordinate Brownian molecular dynamics simulations were performed for a polypeptide chain of

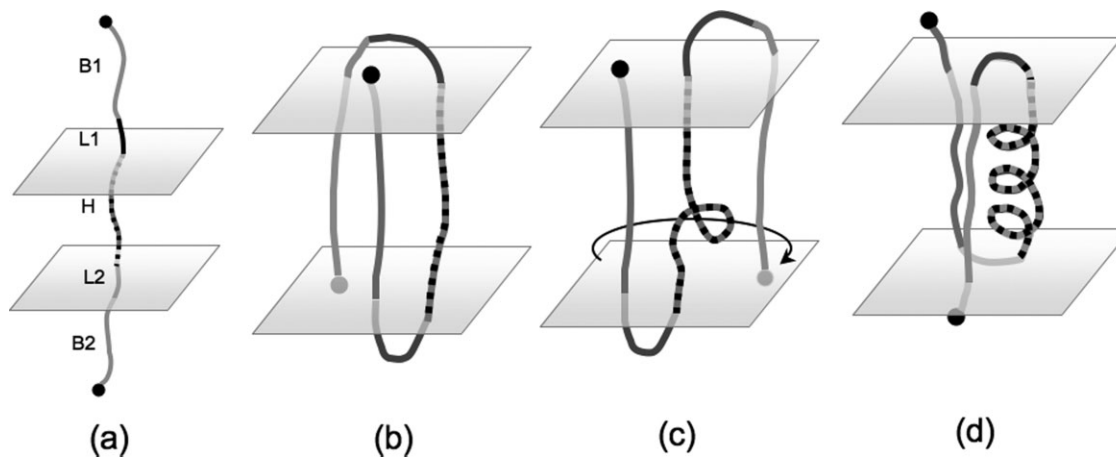


Figure 4. Demonstrative molecular simulations. (a) Initial setup showing five regions and two floor planes. (b) Step 1. Formation of crossover is complete when terminal atoms pass through floor planes. (c) Step 2. When angular torques are applied within the H-segment (dotted), chain ends rotate with respect to each other. (d) Final conformation.

29 residues, all alanines. The forcefield was made as simple as possible to avoid forces that are not relevant to the hypothesis. Bond lengths and angles were constrained to their ideal values by using torsion space equations of motion.²³ The only nonlocal force was van der Waals hard sphere repulsion. No van der Waals attractive term was used. The only local forces were selected backbone angular torques, defined so as to form a helix along one of two possible pathways. A time step, in arbitrary units, was chosen such that no chain crossings were observed and atom–atom collisions were observed to be elastic.

In the following detailed description, we refer to five segments within the chain. They are labeled B1, L1, H, L2, and B2, with segment lengths 7, 3, 9, 3, and 7, respectively. The experiment is illustrated in Figure 4. A total of 4403 simulations were carried out, each as described later.

Step 1. Crossover formation. The chain was initialized with all residues in a randomized extended

conformation ($\psi = 100 \pm 10$, $\phi = -120 \pm 10$). With the H, B1, and B2 segments frozen in their starting configuration and L1, L2 unfrozen, atoms in all segments were subjected to random forces and hard sphere repulsion. External forces (gravity) were applied to the terminal atoms in B1 and B2 driving these atoms toward planes (floors) through residues at the far end of the H-segment and normal to H as illustrated. When both terminal atoms passed through their respective floors, creating an extended crossover conformation of random handedness, Step 2 was initiated.

Step 2. Helix formation. With all atoms unfrozen, backbone ψ angles within the H-segment were assigned one of two possible ψ gradients, north or south, as illustrated in Figure 5, both driving the backbone ψ angle to the ideal helical value, -57° . At each iteration, the angular shifts for each backbone angle were calculated using torsion space equations of motion²³ based on the random force vectors, hard sphere repulsion, and angular torques. Gravity was

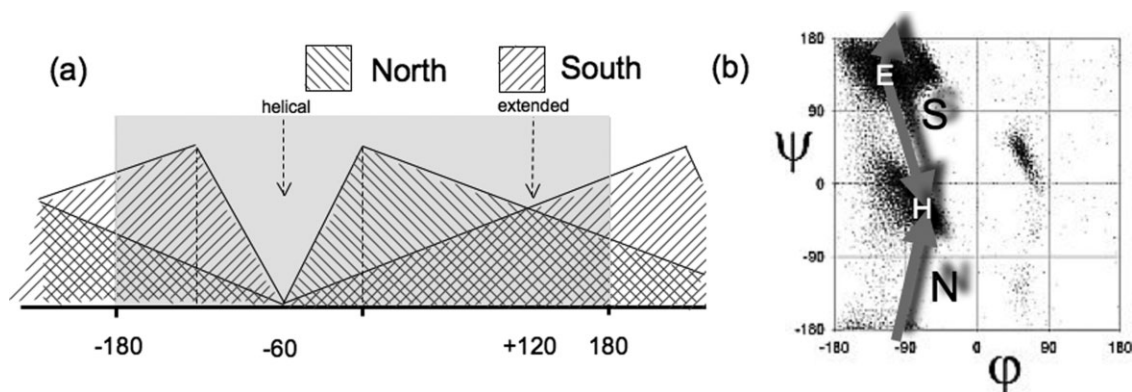


Figure 5. (a) Energy profiles for ψ angle. South: energy profile having maximum at $\psi = -120^\circ$ and minimum at -57° . North: energy profile having maximum at $\psi = 0^\circ$ and minimum at -57° . (b) Ramachandran plot, adapted from Ref. 8, showing north and south pathways to helix and a random sampling database $\phi\psi$ angles. North passes through a sparsely populated zone at $\psi = -120^\circ$. Rotation of ϕ passes through even more sparse zones at $\phi = 0$ and $\phi = 120^\circ$.

switched on to enforce the crossover configuration only if the terminal atoms receded through their respective floor planes, but otherwise no external forces were applied.

An empirical weight was applied to the van der Waals repulsion term that was strong enough that no chain crossings were observed in long simulations, but weak enough that no explosive repulsions were observed. To avoid the complicating effects of local steric interactions on the backbone angle preference, van der Waals forces were calculated only between atoms separated by at least one residue.

Backbone angular torques were applied to the ϕ and ψ angles in the H-region only. Outside of the H-region, backbone angle torques were not used, and any angular shifts were only the results of Cartesian force vectors, including the external “gravity” force. In the H-region, a restraint function was applied to keep the ϕ angle at around $-57^\circ \pm 20^\circ$, but the restraint was applied only if the ϕ and ψ angles were both approaching ideal helical values (geometric mean of ϕ and ψ deviations less than 20°). Despite the lack of a strong restraint on the ϕ angle, the ϕ angle rarely diffused a full 360° in the course of a simulation.

The simulation was carried out for 8000 iterations, after which the results were compiled.

Step 3. Sum statistics. At the end of each simulation, the following values were reported:

- The status of the terminal atoms relative to “floor” planes: “collapsed” or “not collapsed.”
- The final $\phi\psi$ angles of each of the nine residues in the H-segment: “helical” or “not helical.”
- The overall handedness: “right,” “left,” or “ambiguous.”

Acknowledgment

The authors thank Vibin Ramakrishnan for his experimental studies that were not included in this article.

References

1. Richardson JS (1976) Handedness of crossover connections in ss sheets. *Proc Natl Acad Sci USA* 73:2619–2623.
2. Sternberg MJ, Thornton JM (1976) On the conformation of proteins: the handedness of the beta-strand-alpha-helix-beta-strand unit. *J Mol Biol* 105:367–382.
3. Chou KC, Nemethy G, Pottle M, Scheraga HA (1989) Energy of stabilization of the right-handed beta alpha beta crossover in proteins. *J Mol Biol* 205:241–249.
4. Jenkins J, Mayans O, Pickersgill R (1998) Structure and evolution of parallel β -helix proteins. *J Struct Biol* 122:236–246.
5. Westhead DR, Slidel TW, Flores TP, Thornton JM (1999) Protein structural topology: automated analysis and diagrammatic representation. *Protein Sci* 8:897–904.
6. Wilks SS (1962) *Mathematical statistics*. New York: Wiley.
7. Ramakrishnan C, Ramachandran GN (1965) Stereochemical criteria for polypeptide and protein chain conformations. II. Allowed conformations for a pair of peptide units. *Biophys J* 5:909.
8. Ho BK, Thomas A, Brasseur R (2003) Revisiting the Ramachandran plot: hard-sphere repulsion, electrostatics, and H-bonding in the alpha-helix. *Protein Sci* 12:2508–2522.
9. Zaman MH, Shen MY, Berry RS, Freed KF, Sosnick TR (2003) Investigations into sequence and conformational dependence of backbone entropy, inter-basin dynamics and the flory isolated-pair hypothesis for peptides. *J Mol Biol* 331:693–711.
10. Baxa MC, Freed KF, Sosnick TR (2008) Quantifying the structural requirements of the folding transition state of protein A and other systems. *J Mol Biol* 381:1362–1381.
11. Murzin AG, Brenner SE, Hubbard T, Chothia C (1995) SCOP: a structural classification of proteins database for the investigation of sequences and structures. *J Mol Biol* 247:536–540.
12. Sippl MJ (1993) Boltzmann’s principle, knowledge-based mean fields and protein folding. An approach to the computational determination of protein structures. *J Comput-Aided Mol Des* 7:473–501.
13. Hao MH, Scheraga HA (1999) Designing potential energy functions for protein folding. *Curr Opin Struct Biol* 9:184–188.
14. Buck P, Bystroff C (2008) Simulating protein folding initiation sites using an alpha-carbon-only knowledge-based forcefield. *Proteins* 76:331–342.
15. Bystroff C, Baker D (1998) Prediction of local structure in proteins using a library of sequence-structure motifs. *J Mol Biol* 281:565–577.
16. Voelz VA, Shell MS, Dill KA (2009) Predicting peptide structures in native proteins from physical simulations of fragments. *PLoS Comput Biol* 5:e1000281.
17. Bystroff C, Garde S (2003) Helix propensities of short peptides: molecular dynamics versus bioinformatics. *Proteins* 50:552–562.
18. Yi Q, Bystroff C, Rajagopal P, Klevit RE, Baker D (1998) Prediction and structural characterization of an independently folding substructure in the src SH3 domain. *J Mol Biol* 283:293–300.
19. Blanco FJ, Rivas G, Serrano L (1994) A short linear peptide that folds into a native stable bold beta-hairpin in aqueous solution. *Nat Struct Biol* 1:584–590.
20. Mallam AL, Morris ER, Jackson SE (2008) Exploring knotting mechanisms in protein folding. *Proc Natl Acad Sci USA* 105:18740.
21. Taylor WR (2000) A deeply knotted protein structure and how it might fold. *Nature (London)* 406:916–919.
22. Hobohm U, Sander C (1994) Enlarged representative set of protein structures. *Protein Sci* 3:522–524.
23. Bystroff C (2001) An alternative derivation of the equations of motion in torsion space for a branched linear chain. *Protein Eng* 14:825.